The MYB96 Transcription Factor Mediates Abscisic Acid Signaling during Drought Stress Response in Arabidopsis[1][W]

Pil Joon Seo[2], Fengning Xiang[2], Meng Qiao, Ju-Young Park, Young Na Lee, Sang-Gyu Kim, Yong-Hwan Lee, Woong June Park, and Chung-Mo Park*

Molecular Signaling Laboratory, Department of Chemistry (P.J.S., S.-G.K., C.-M.P.), Department of Agricultural Biotechnology and Center for Fungal Pathogenesis (J.-Y.P., Y.-H.L.), and Plant Genomics and Breeding Institute (C.-M.P.), Seoul National University, Seoul, Korea 151–742; Key Laboratory of Plant Cell Engineering and Germplasm Innovation, School of Life Sciences, Shandong University, Jinan 250100, Shandong, China (F.X., M.Q.); and Department of Molecular Biology, Brain Korea 21 Graduate Program for RNA Biology, Institute of Nanosensor and Biotechnology, Dankook University, Yongin, Korea 448–701 (Y.N.L., W.J.P.)

Plant adaptive responses to drought are coordinated by adjusting growth and developmental processes as well as molecular and cellular activities. The root system is the primary site that perceives drought stress signals, and its development is profoundly affected by soil water content. Various growth hormones, particularly abscisic acid (ABA) and auxin, play a critical role in root growth under drought through complex signaling networks. Here, we report that a R2R3-type MYB transcription factor, MYB96, regulates drought stress response by integrating ABA and auxin signals. The *MYB96*-mediated ABA signals are integrated into an auxin signaling pathway that involves a subset of *GH3* genes encoding auxin-conjugating enzymes. A *MYB96*-overexpressing Arabidopsis (*Arabidopsis thaliana*) mutant exhibited enhanced drought resistance with reduced lateral roots. In the mutant, while lateral root primordia were normally developed, meristem activation and lateral root elongation were suppressed. In contrast, a T-DNA insertional knockout mutant was more susceptible to drought. Auxin also induces *MYB96* primarily in the roots, which in turn induces the *GH3* genes and modulates endogenous auxin levels during lateral root development. We propose that *MYB96* is a molecular link that mediates ABA-auxin cross talk in drought stress response and lateral root growth, providing an adaptive strategy under drought stress conditions.

Water availability in the soil influences virtually all aspects of plant architecture and physiology. Consequently, the root system is very sensitive to water deficit. Under drought stress conditions, depth and elongation of the primary root and formation of the lateral roots are adjusted to sustain the viability of plants (Horvath et al., 2003; Deak and Malamy, 2005; Gubler et al., 2005; Yu et al., 2008). Notably, while primary root growth is not discernibly affected by water deficit, the number of lateral roots and their growth are significantly reduced (Deak and Malamy, 2005).

Lateral root formation is initiated when a few pericycle founder cells adjacent to the two xylem poles divide anticlinically and asymmetrically, resulting in two shorter cells flanked by two longer cells (Dubrovsky et al., 2000; Casimiro et al., 2003; De Smet et al., 2008). This step is referred to as lateral root initiation. The daughter cells undergo several rounds of cell division, which result in a dome-shaped lateral root primordium that subsequently emerges through the outer cell layers (referred to as emergence of lateral root primordium). The lateral root primordium further expands through cell divisions after lateral root primordial emergence, and a meristem is established when three to five cell layers are formed within the lateral root primordium (Casimiro et al., 2003). The lateral root meristem is activated when the soil conditions are favorable.

The developmental steps during lateral root formation can be traced at the molecular level. The G1-S transition of the cell cycle in the pericycle founder cells is regulated by Kip-related protein2 (KRP2), functioning as a cyclin-dependent kinase inhibitor (Himanen et al., 2002). The *KRP2* gene is repressed by auxin but activated by abscisic acid (ABA), which is consistent with the promotive role of auxin and the repressive role of ABA in lateral root initiation (Verkest et al.,

[1] This work was supported by the Brain Korea 21, Biogreen 21 (grant no. 20080401034001), and National Research Laboratory programs, by the Plant Signaling Network Research Center (grant no. 2009–0079297) and the Korea Science and Engineering Foundation (grant no. 2007–03415), and by the National Special Science Research Program of China (grant no. 2007CB948203 to F.X.).

[2] These authors contributed equally to the article.

* Corresponding author; e-mail cmpark@snu.ac.kr.

The author responsible for distribution of materials integral to the findings presented in this article in accordance with the policy described in the Instructions for Authors (www.plantphysiol.org) is: Chung-Mo Park (cmpark@snu.ac.kr).

[W] The online version of this article contains Web-only data.
www.plantphysiol.org/cgi/doi/10.1104/pp.109.144220

2005; De Smet et al., 2006). Several ABA-related genes, such as *9-CIS-EPOXYCAROTENOID DIOXYGENASE9* (*NCED9*), encoding an ABA biosynthetic enzyme (Taylor et al., 2000), are also closely related to the process of lateral root initiation (Tan et al., 2003; De Smet et al., 2006).

Lateral root formation is greatly influenced by both endogenous and external stimuli. The activation of the lateral root meristem occurs with the help of a series of ABA-responsive genes. In the presence of ABA, lateral root formation is inhibited, although the dome-shaped primordium is normally developed. This inhibition is caused by the ABA-mediated repression of the activation of newly established lateral root meristem (De Smet et al., 2006). Meanwhile, it has been shown that the *ABA insensitive8* (*abi8*) mutant is incapable of maintaining meristem activity (Brocard-Gifford et al., 2004), which is in contrast to the inhibitory role of ABA in lateral root formation. Although it has not been experimentally examined, one possibility would be that some lateral root initiation genes might represent molecular events occurring in the surrounding cells, which are still required for normal lateral root initiation (De Smet et al., 2003; Tan et al., 2003). External signals mediated by environmental factors, such as drought and osmotic stress (Deak and Malamy, 2005) and soil nutrients (Malamy and Ryan, 2001; Little et al., 2005), are also integrated into the growth hormone signaling networks (Ivanchenko et al., 2008).

Auxin is known to promote the entire process of lateral root formation. It plays a primary role in lateral root initiation (Xie et al., 2000, 2002; Ljung et al., 2002; Dubrovsky et al., 2008). In contrast, under drought or osmotic stress conditions, the lateral root meristem activation is suppressed by ABA-mediated signals, producing fewer and shorter lateral roots (De Smet et al., 2003; Deak and Malamy, 2005). Auxin is also involved in the meristem activity of the lateral roots, as has been shown with a mutation in the *ABERRANT LATERAL ROOT FORMATION3* gene (Celenza et al., 1995). Lateral root growth is blocked after the emergence of the lateral root primordium in the mutant, which also occurs in the lateral roots of ABA-treated plants or of plants grown under drought conditions (De Smet et al., 2003; Deak and Malamy, 2005), suggesting that signaling cross talk occurs between ABA and auxin. It is generally believed that ABA regulates lateral root formation by modulating auxin signaling pathways (De Smet et al., 2003; Deak and Malamy, 2005). However, the underlying molecular mechanisms have not yet been explored at the molecular level.

In this work, we examined morphological and molecular aspects of an Arabidopsis (*Arabidopsis thaliana*) activation-tagged mutant, *myb96-ox*, in which the *MYB96* gene is constitutively overexpressed. While the *myb96-ox* mutant exhibited enhanced resistance to drought with stunted growth and reduced lateral roots, a T-DNA insertional knockout mutant, *myb96-1*, was more sensitive to water deficit. Notably, the *MYB96*-mediated ABA signals are transduced through an auxin signaling pathway that involves a subset of *GH3* genes. These signals regulate lateral root formation by arresting the meristem activity after the emergence of lateral root primordium, providing a means of controlling root branching under drought conditions (Horvath et al., 2003; Gubler et al., 2005).

RESULTS

myb96-ox Exhibits Dwarfed Growth with Reduced Lateral Roots

By screening an *Arabidopsis* activation-tagged mutant pool generated by randomly integrating the cauliflower mosaic virus (CaMV) 35S enhancer element into the genome of ecotype Columbia (Col-0), we isolated the morphogenic mutant *myb96-ox* that exhibits dwarfed growth with altered leaf morphology (Fig. 1A). The *myb96-ox* leaves were small and severely curled downward with an asymmetric axis (Fig. 1B). The root system was also affected in the mutant. While the primary root growth was apparently normal (Supplemental Fig. S1), the growth of lateral roots was significantly reduced (Fig. 1C) with lower lateral root density (Fig. 1D). Overall, the *myb96-ox* phenotypes were quite similar to those observed in plants grown under abiotic stress conditions (Heil and Baldwin, 2002), suggesting that the tagged gene might be involved in abiotic stress responses.

Mapping the T-DNA insertional site using a three-step thermal asymmetric interlaced-PCR (Liu et al., 1995) and gene expression analysis revealed that a gene (At5g62470) encoding a MYB transcription factor, MYB96, was activated by the nearby insertion of the enhancer element in the mutant (Fig. 1, E and F). Transgenic plants overexpressing the *MYB96* gene under the control of the CaMV 35S promoter recapitulated the *myb96-ox* phenotypes (Fig. 1, A and B), indicating that the overexpression of *MYB96* is the molecular cause of the *myb96-ox* phenotypes. The T-DNA insertional knockout mutant *myb96-1* was phenotypically indistinguishable from wild-type plants when grown under normal growth conditions (Fig. 1A). However, it exhibited an altered response to water deficit, which was efficiently rescued by the expression of a genomic DNA segment containing the *MYB96* gene and its own promoter (see Fig. 3G below), confirming the interconnectedness of *MYB96* and the *myb96-ox* phenotypes.

The MYB96 protein consists of 352 amino acids (Supplemental Fig. S2). Protein structure analysis revealed that it belongs to the R2R3-type MYB subfamily with two imperfect repeats (R1 and R2), each consisting of approximately 53 residues that form a typical helix-turn-helix configuration (Stracke et al., 2001).

MYB96 Is Induced by ABA and Drought

To examine the subcellular localization of the MYB96 protein, a GFP-coding sequence was fused in

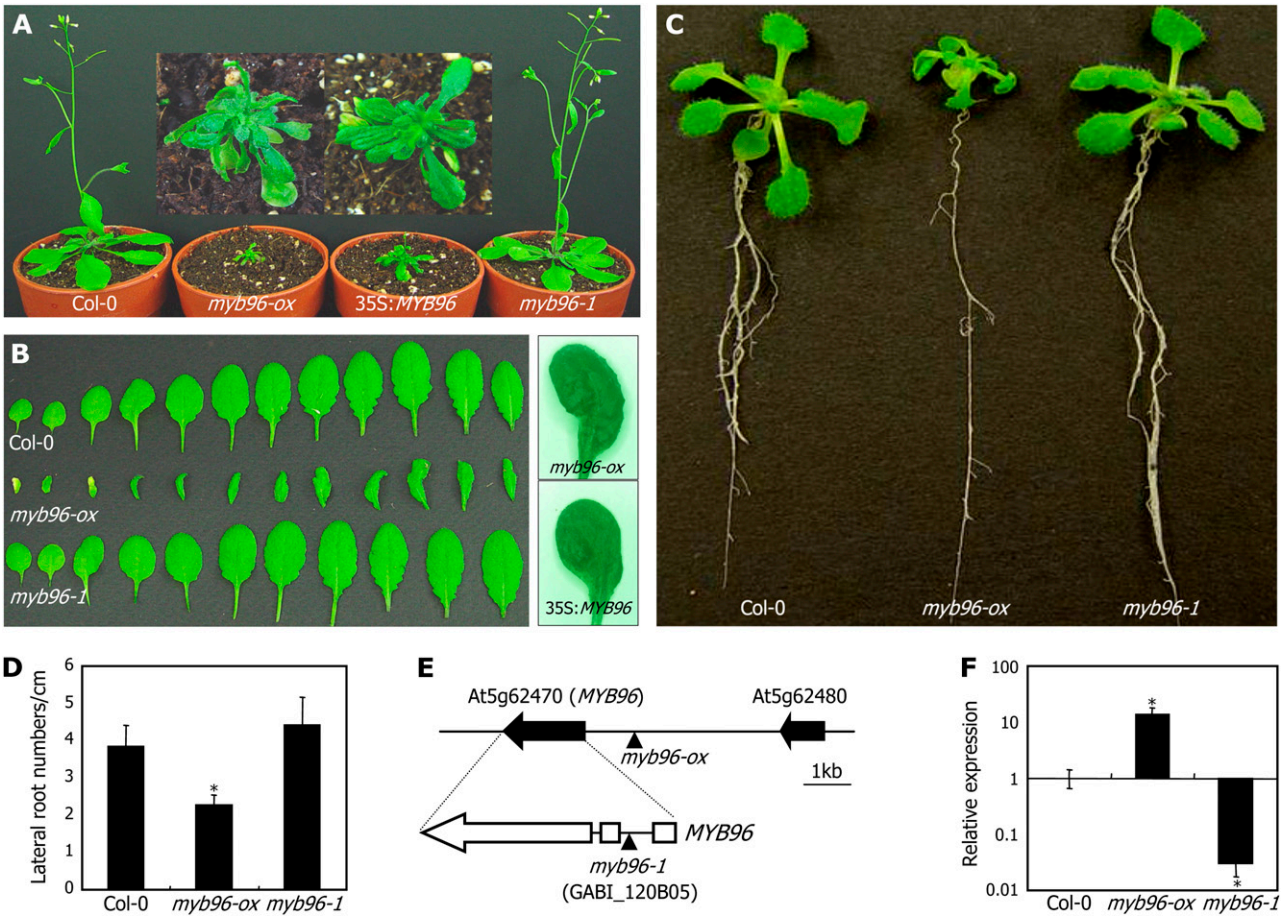

Figure 1. *myb96-ox* exhibits dwarfed growth with altered leaf shape and reduced lateral roots. A, Phenotypes of *myb96-ox* and *myb96-1*. Four-week-old plants grown in soil were photographed. Transgenic plants overexpressing *MYB96* under the control of the CaMV 35S promoter (35S:*MYB96*) were included for comparison. The insets are enlarged views of the *myb96-ox* and 35S:*MYB96* plants. B, Comparison of leaf morphologies. The rosette leaves were photographed. A rosette leaf of the 35S:*MYB96* plants was also included as a comparison (at right). C, Root phenotypes. Plants were grown on vertical MS agar plates for 3 weeks. D, Lateral root densities. Lateral root density was calculated by dividing the lateral root number by the primary root length. Visible lateral roots of 20 plants were counted and averaged for each plant group. Error bars represent SE. Statistical significance of the measurements was determined by Student's *t* test (* $P < 0.01$). E, Mapping of T-DNA insertion sites in *myb96-ox* and *myb96-1*. Black arrows indicate gene loci. The white arrow indicates exons of the *MYB96* gene. F, Transcript levels of *MYB96* in *myb96-ox* and *myb96-1*. Transcript levels were determined by qRT-PCR using RNA samples extracted from 2-week-old whole plants grown on MS agar plates. Biological triplicates were averaged. Error bars represent SE (*t* test; * $P < 0.01$). The *y* axis is presented on a logarithmic scale for better comparison of fold changes.

frame to the 3′ end of the *MYB96* gene, and the fusion construct was transiently expressed in onion (*Allium cepa*) epidermal cells. The fusion was exclusively detected in the nucleus (Fig. 2A), which is consistent with its role as a transcription factor.

While the *MYB96* gene was expressed at a high level in the leaves and flowers, it was expressed at a relatively lower level in the roots (Fig. 2B). In addition, it was expressed throughout the plant life (Fig. 2C). To further examine the localized expression patterns in different plant tissues, a promoter sequence covering an approximately 2-kb region upstream of the *MYB96* transcription start site was fused to a GUS-coding sequence, and the promoter-GUS reporter was transformed into wild-type plants. GUS activity was detected at a high level in the leaves and hypocotyls (Fig. 2D), consistent with the gene expression profiling (Fig. 2B). Although the activity was low in the roots, including the primary root tips, high GUS activity was detected in lateral root primordia (Fig. 2D). The overall level of GUS activity was high in the leaves. Notably, more close examination revealed that it was localized mainly into the guard cells.

The *myb96-ox* phenotypes were similar to those observed in plants grown under environmental stress conditions. In addition, the high expression of *MYB96* in the guard cells was similar to the expression patterns of some genes mediating abiotic stress responses (Zhang et al., 2007; Jung et al., 2008). Therefore, we examined the effects of various environmental condi-

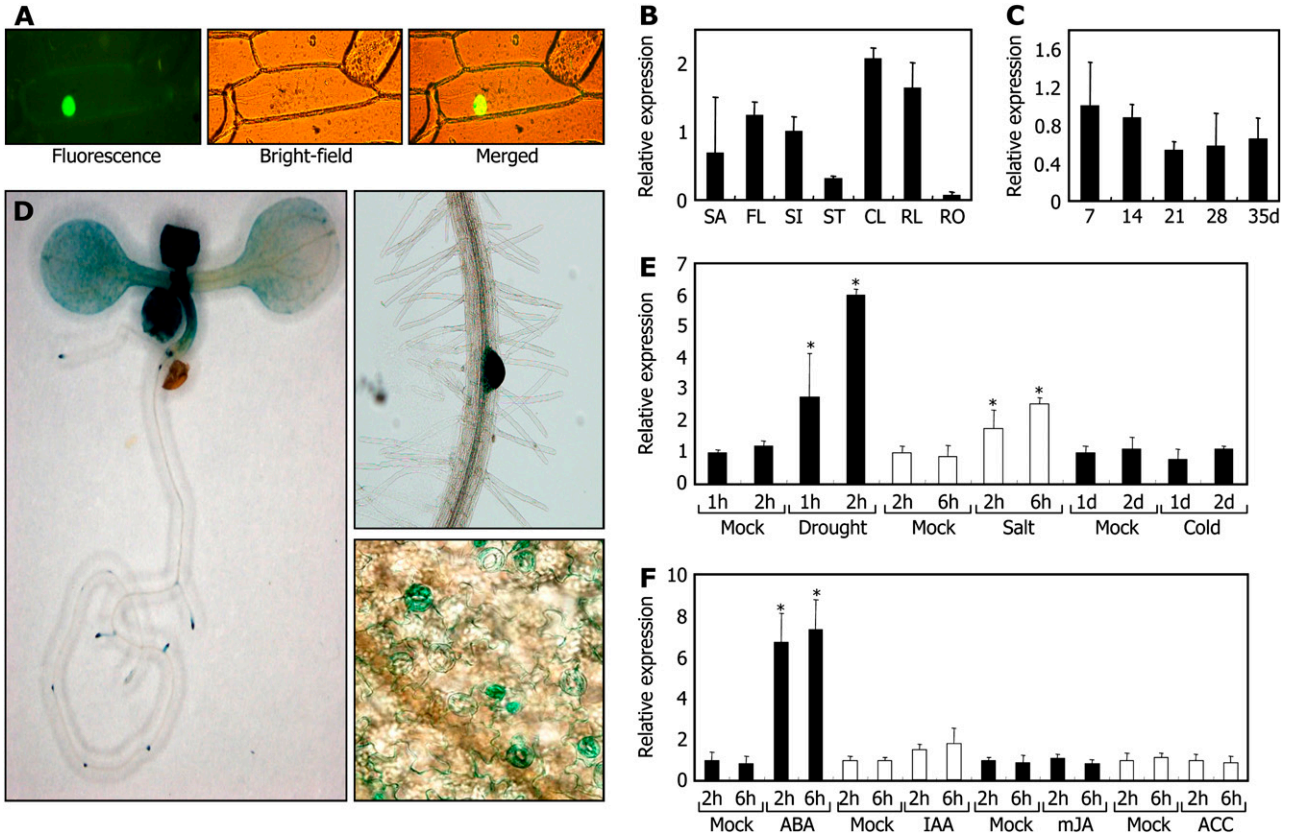

Figure 2. MYB96 is induced by ABA and drought. In B, C, E, and F, transcript levels were determined as described in Figure 1F. A, Nuclear localization of MYB96 protein. A MYB96-GFP fusion was transiently expressed in onion epidermal cells and visualized by bright-field and fluorescence microscopy. B, Tissue-specific expression of MYB96. SA, Shoot apical region; FL, flowers; SI, siliques; ST, stems; CL, cauline leaves; RL, rosette leaves; RO, roots. Error bars represent SE. C, Growth stage-dependent expression of MYB96. Whole plants harvested at the indicated time points were used for RNA extraction. d, Days after cold imbibition. Error bars represent SE. D, Distribution of pMYB96-GUS expression in plant tissues. GUS activity was assayed in the whole plant (left), in the lateral root primordium (right, top), and in the guard cells (right, bottom). E and F, Effects of abiotic stresses (E) and growth hormones (F) on MYB96 expression. Two-week-old plants grown on MS agar plates were used for the treatments. Error bars represent SE (*t* test; * $P < 0.01$). h, Hours; d, days. ABA, IAA, and mJA were used at 20 μM, ACC was used at 50 μM, and NaCl was used at 200 mM.

tions on *MYB96* expression. The *MYB96* gene was induced significantly by drought (Fig. 2E). It was also induced moderately by high salt. Furthermore, *MYB96* expression was significantly elevated by ABA but unaffected by methyl jasmonic acid (mJA) and 1-aminocyclopropane-1-carboxylic acid (ACC; Fig. 2F). Indole-3-acetic acid (IAA) also induced *MYB96* expression by approximately 1.8-fold (see Fig. 5A below). These observations suggest that *MYB96* may play a role in ABA-mediated drought stress response.

MYB96 Enhances ABA-Mediated Drought Resistance

Our data suggested that the *MYB96*-overexpressing *myb96-ox* mutant and the knockout *myb96-1* mutant would respond to drought differentially from wild-type plants. As expected, whereas the *myb96-ox* mutant showed enhanced resistance to drought, the *myb96-1* mutant was susceptible to drought (Fig. 3A). Measurements of the rate of water loss from the leaves also showed similar results. The water content of the *myb96-1* leaves rapidly decreased upon exposure to drought (Fig. 3B). The rate of water loss in the *myb96-ox* leaves was not discernibly different from that in the wild-type leaves. This could be due to the small size of the *myb96-ox* leaves and thus the small total volume of water in it.

To look into the molecular mechanisms underlying the function of MYB96 in drought resistance, we searched for genes whose expression levels were altered in the *myb96-ox* and *myb96-1* mutants. Most of the stress genes examined, except for the dehydration-responsive gene *RESPONSIVE TO DEHYDRATION22* (*RD22*; Yamaguchi-Shinozaki and Shinozaki, 1993), were unaffected by the *myb96* mutations (Supplemental Fig. S3). The *RD22* expression was elevated by approximately 12-fold in the *myb96-ox* mutant but reduced by 3- to 4-fold in the *myb96-1* mutant (Fig. 3C),

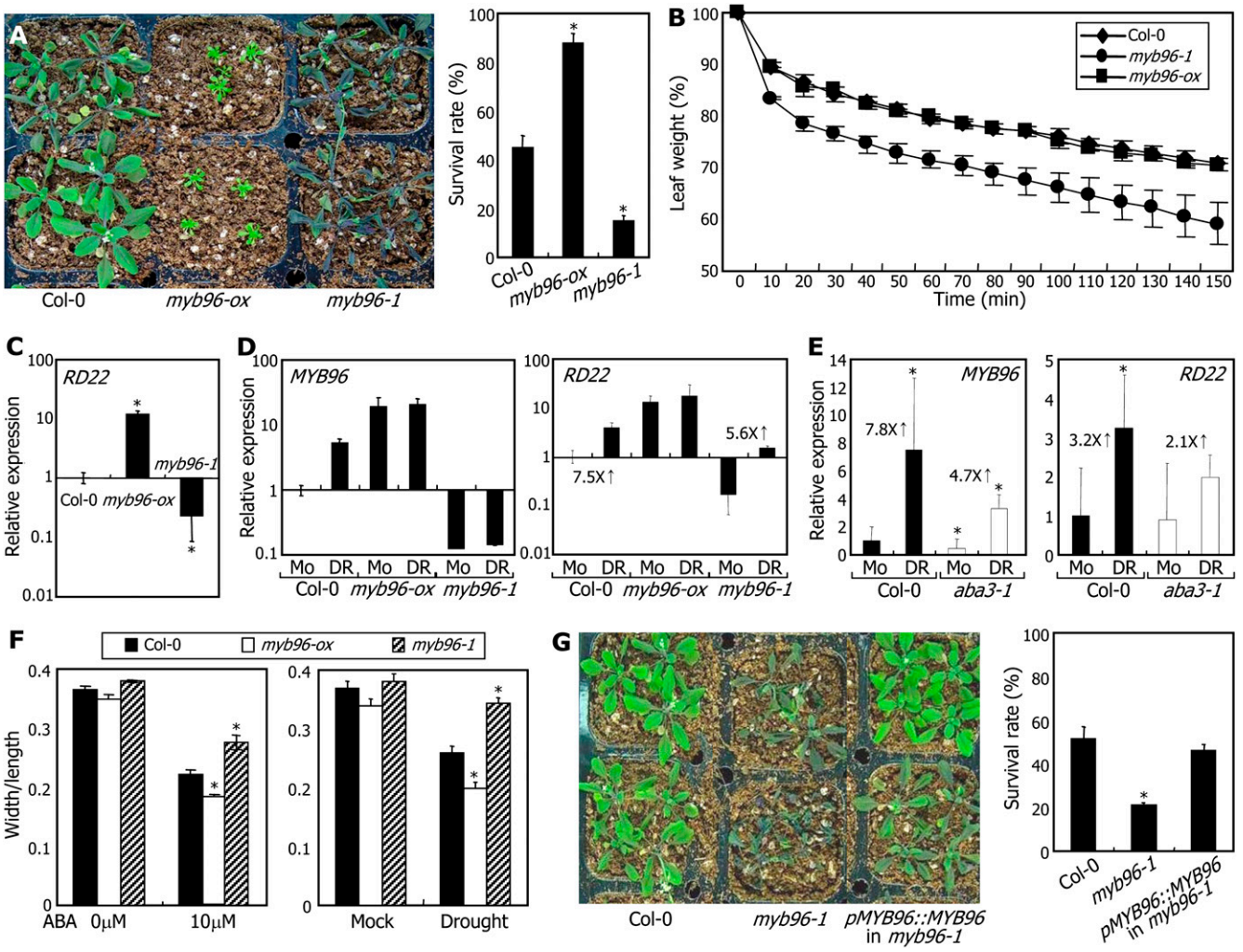

Figure 3. *MYB96* regulates drought resistance through the ABA signaling pathway. In C to E, transcript levels were determined as described in Figure 1F. Two-week-old whole plants grown on MS agar plates were used for RNA extraction. In C and D, the *y* axis is presented on a logarithmic scale for better comparison of fold changes. Mo, Mock; DR, drought. A, Drought stress responses of *myb96-ox* and *myb96-1*. To measure survival rates, three independent measurements, each consisting of 30 seedlings, were averaged for each plant group. Error bars represent SE (*t* test; * $P < 0.01$). B, Water loss assays. The leaves of 4-week-old plants were used. Leaves from seven plants were measured and averaged. C, Transcript levels of *RD22* in *myb96-ox* and *myb96-1*. Error bars represent SE (*t* test; * $P < 0.05$). D, Effects of drought on expression of *MYB96* and *RD22*. Error bars represent SE. E, Expression of *MYB96* and *RD22* in *aba3-1*. Error bars represent SE (*t* test; * $P < 0.01$). F, Stomatal apertures in the *myb96-ox* and *myb96-1* leaves. Two-week-old plants grown on MS agar plates were incubated in MS liquid cultures supplemented with 10 μM ABA for 6 h (left). Two-week-old plants grown in soil were also subjected to drought treatments for 2 weeks before measuring stomatal apertures (right). Approximately 20 stomatal openings on the fourth leaves were measured and averaged. Error bars represent SE of the mean (*t* test; * $P < 0.05$). G, Complementation assays on *myb96-1*. A *MYB96* gene with its own promoter was transformed into *myb96-1*. Survival rates were measured as described in A. Error bars represent SE (*t* test; * $P < 0.01$).

indicating that *MYB96* is required for proper expression of *RD22*. *RD22* was still induced by drought in the *myb96-1* mutant (Fig. 3D). However, the transcript level was significantly lower than that in wild-type plants exposed to drought, showing that *MYB96*, at least partially, mediates drought induction of *RD22*. We next examined whether drought induction of *MYB96* depends on ABA. The effect of drought on the expression of *MYB96* was significantly reduced in the ABA-deficient *aba3-1* mutant, as it was on the expression of *RD22* (Fig. 3E), sustaining the hypothesis that *MYB96* is induced by drought along an ABA-dependent signaling pathway.

To examine whether the responses of the *myb96-ox* and *myb96-1* mutants to drought are related to the regulation of the stomatal opening, stomatal apertures were measured in the leaves. Whereas the stomatal aperture decreased to a greater degree in the ABA-treated *myb96-ox* leaves than in the wild-type leaves, it decreased to a lesser degree in the ABA-treated *myb96-1*

leaves (Fig. 3F, left). The differential stomatal apertures between the *myb96-ox* and *myb96-1* leaves were more evident when the plants were treated with drought (Fig. 3F, right), indicating that *MYB96*-mediated signals enhance plant resistance to drought by reducing stomatal opening. However, stomatal densities of the abaxial surfaces of the *myb96-ox* and *myb96-1* leaves were essentially similar to that in the wild-type leaves (Supplemental Fig. S4), showing that MYB96 regulates specifically stomatal opening.

To confirm the role of *MYB96* in ABA-mediated drought resistance, the *myb96-1* mutant was transformed with a wild-type *MYB96* gene driven by its own promoter. The *pMYB96*::*MYB96* in *myb96-1* transgenic plants were as resistant to drought as wild-type plants were (Fig. 3G), verifying the role of *MYB96* in drought resistance.

ABA Responsiveness Is Altered in Seed Germination and Lateral Root Formation of *myb96-ox*

We also examined other plant responses mediated by ABA, such as seed germination and lateral root formation, in the *myb96-ox* and *myb96-1* mutants. We found that the germination process of the *myb96-ox* seeds was hypersensitive to ABA (Fig. 4A). It was considerably delayed in the presence of 5 μM ABA. In contrast, germination of the *myb96-1* seeds was slightly but reproducibly more resistant to ABA (see below).

The most prominent phenotype of the *myb96-ox* mutant was reduced lateral roots (Figs. 1C and 4B). To more systematically evaluate the effects of ABA, the mutant plants were grown on vertical half-strength Murashige and Skoog (MS) agar plates (MS agar plates hereafter) supplemented with various concentrations of ABA (0–5 μM). Whereas lateral roots were reduced by only approximately 20% in the presence of 0.5 μM ABA in wild-type plants, they were reduced by more than 70% in the *myb96-ox* mutant under the same conditions (Fig. 4B), demonstrating that *MYB96* might be related to ABA signaling in regulating lateral root formation.

Lateral root formation of the *myb96-1* knockout mutant was still responsive to ABA (Fig. 4B). It was also indistinguishable from that of wild-type plants in the presence of mannitol, which mimics drought conditions (Fig. 4C). The marginal differences upon ABA treatment on seed germination and lateral root growth in the *myb96-1* mutant might be due to some functional redundancy of the MYB proteins or multiple ABA signaling pathways governing seed germination and lateral root development.

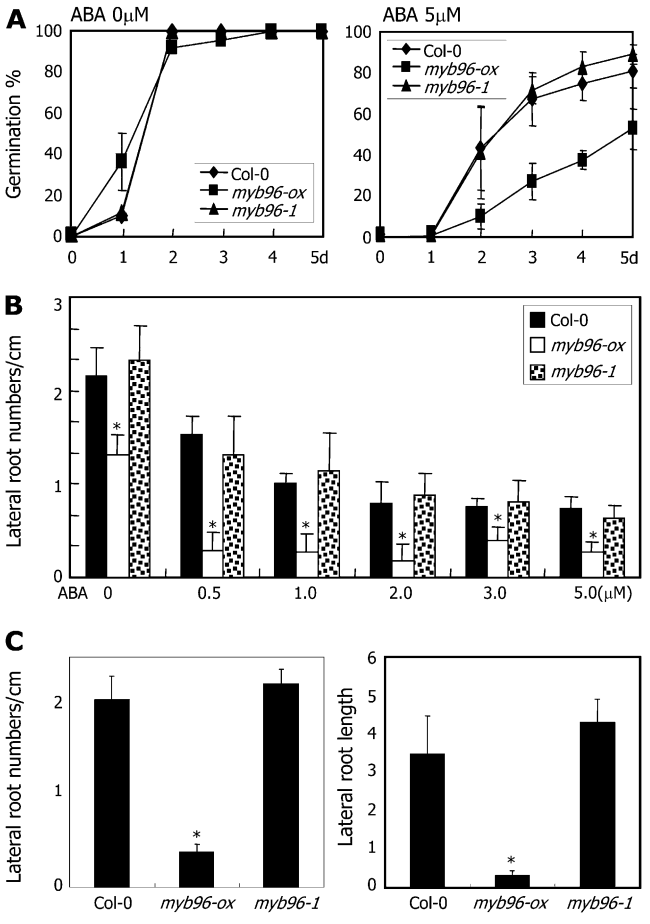

Figure 4. Seed germination and lateral root formation of *myb96-ox* are hypersensitive to ABA. A, Seed germination rates in the presence of 5 μM ABA. Fifty seeds were germinated and counted for each seed group. Three measurements were averaged. Error bars represent SE. Radicle emergence was used as a morphological marker for germination. d, Days after cold imbibition. B, Effects of ABA on lateral root formation. Plants were grown as in A, but MS agar plates supplemented with 0 to 5 μM ABA were used. Visible lateral roots of 20 seedlings were counted and averaged. Error bars represent SE (*t* test; * $P < 0.01$). C, Lateral root formation of *myb96-ox* and *myb96-1* in the presence of 100 mM mannitol. For mannitol treatments, seedlings were grown at 22°C for 3 d on MS agar plates after cold imbibition, transferred to vertical MS agar plates supplemented with 100 mM mannitol, and further grown for 2 weeks. Visible lateral roots of 30 plants were counted and averaged. Error bars represent SE (*t* test; * $P < 0.01$).

MYB96-Mediated ABA Signals Are Incorporated into an Auxin Signaling Pathway

Auxin and ABA are two major growth hormones governing lateral root development. Accumulating evidence suggests that a physiological balance between the auxin-promotive and ABA-repressive signals is crucial for the emergence of lateral root primordium and lateral root meristem activation (Deak and Malamy, 2005; De Smet et al., 2006).

To examine whether the *MYB96*-mediated ABA signals are linked to auxin signaling during lateral root development, we examined the effects of auxin on *MYB96* expression using transgenic plants overexpressing a gene fusion in which the *MYB96* gene promoter sequence was fused to a GUS-coding sequence (*pMYB96-GUS*). Interestingly, whereas the level of GUS activity was not detectably influenced by IAA in the aerial plant parts, the level was signif-

icantly elevated in the roots (Fig. 5A). In untreated roots, it was detected primarily in the tips of lateral roots and in the lateral root primordium (Figs. 2D and 5A). The domain of GUS activity was extended throughout the whole root system after IAA treatments, mainly in the vasculature of the primary root, indicating that auxin up-regulates *MYB96* expression mostly in the roots.

Treatments with ABA exhibited distinct induction patterns of *MYB96*. GUS activity was elevated broadly in the aerial plant parts (Supplemental Fig. S5, A and B). In the roots, it was induced primarily in the emerging lateral roots. When the transgenic plants were treated with both IAA and ABA, GUS activity was elevated in the emerging lateral roots as in the ABA-treated seedlings. However, the level in the vasculature of the primary root was lower than that in the vasculature of the IAA-treated roots (Supplemental Fig. S5, B and C). Based on previous observations (Himanen et al., 2002; De Smet et al., 2003) and our own observations, it was concluded that ABA inhibits the action of IAA on pericycle cell division rather than the effects of IAA on *MYB96* expression. As a result, fewer primordia are produced in the presence of ABA, which in turn results in fewer cells expressing *MYB96*. Consistent with this, *MYB96* was induced specifically in the pericycle cells of the primary root treated with IAA for 6 h (Supplemental Fig. S6).

A subset of *GH3* genes encoding a subset of IAA-conjugating enzymes is reportedly induced by ABA and abiotic stresses (Mallory et al., 2005; Park et al., 2007). Furthermore, *GH3*-overexpressing mutants show dwarfed growth with altered leaf morphology and reduced lateral roots (Mallory et al., 2005; Sorin et al., 2005; Park et al., 2007), which are strikingly similar to the *myb96-ox* phenotypes.

Therefore, we investigated whether *MYB96* is related to the *GH3*-mediated responses to abiotic stresses. Expression of the *GH3* genes and their upstream regulators, such as *AUXIN RESPONSE FACTOR* (*ARF*) genes, was examined in the *myb96-ox* and *myb96-1* mutants. Among the six *GH3* genes (*GH3-1*–*GH3-6*) examined, *GH3-3*, *GH3-5*/*WES1*, and *GH3-6*/*DFL1* were up-regulated by more than 2-fold in the *myb96-ox* mutant (Fig. 5B), while other *GH3* genes were not discernibly affected. Expression of *ARF17* was also elevated in the mutant. However, no visible changes in the expression of other genes involved in auxin signal perception and signaling, including *TRANSPORT INHIBITOR RESPONSE1*, *ARF5*, and *ARF7*, were observed in the *myb96-ox* and *myb96-1* mutants (Supplemental Fig. S7).

We next examined the effects of ABA on the expression of the *GH3* and *ARF* genes in the shoots and roots. *MYB96* was expressed to a similar level in the shoots and roots of 2-week-old plants (Fig. 5C), which is in contrast to the relatively low-level expression in the roots of fully grown plants (Fig. 2B). Analysis of *MYB96* transcript levels throughout the plant growth stages revealed that the transcript level was drastically reduced 3 weeks after germination (Supplemental Fig. S8). *MYB96* was induced by ABA in both the shoots and roots but with higher induction in the latter (Fig. 5C). *GH3-3* and *GH3-5* were induced by ABA to a higher level in the roots than in the shoots. While *RD22* expression was relatively higher in the shoots, it was induced by ABA to a similar degree in both the roots and shoots, which would be related to the role of *RD22* in *MYB96*-mediated drought resistance (Fig. 3).

ARF17 does not seem to be directly related to *MYB96* regulation of the *GH3* genes. It was induced by ABA only slightly in both the shoots and roots (Fig. 5C). In addition, kinetic comparison of the *ARF17* and *GH3-5* expression patterns revealed that *GH3-5* was induced earlier than *ARF17* after ABA treatments (Supplemental Fig. S9). Collectively, these observations strongly support the hypothesis that the *MYB96*-mediated ABA signals are modulated through an auxin signaling pathway, which would affect auxin metabolism as observed in the *GH3*-overexpressing mutants (Park et al., 2007).

ABA Induction of *GH3-3* and *GH3-5* Genes Depends on *MYB96*

The selected *GH3* genes are up-regulated in the *myb96-ox* mutant (Fig. 5B). The *MYB96* gene is induced by auxin in the roots (Fig. 5A). Therefore, we asked whether the auxin induction of the *GH3* genes requires *MYB96* in the roots and how the ABA and auxin signals are interconnected. We found that the *GH3* genes were still induced efficiently by IAA in the *myb96-ox* and *myb96-1* roots, reaching levels comparable to that in wild-type plants (Fig. 6A), indicating that auxin induction of the *GH3* genes is independent of *MYB96*.

We next examined whether the *GH3* genes would be induced by ABA in a *MYB96*-dependent manner specifically in the roots. The *myb96-ox* and *myb96-1* mutants were treated with ABA, and the expression patterns of the *GH3* genes were examined in the roots. We observed that whereas ABA induction of *GH3-3* and *GH3-5* was significantly reduced in the *myb96-1* mutant, that of *GH3-6* was not (Fig. 6B).

Meanwhile, the *RD22* gene was unaffected by auxin, and its transcript levels were unchanged in the *WES1*-overexpressing (*wes1-D*) and *WES1*-deficient (*wes1-1*) mutants (Supplemental Fig. S10; Park et al., 2007), supporting that *MYB96-GH3* signaling is independent of *RD22*-mediated signaling.

We also examined whether the *myb96-ox* root phenotypes were rescued by IAA. The number of lateral roots increased to a discernible level in the presence of IAA higher than 0.1 μM in the *myb96-ox* mutant (Fig. 6C). However, it was not fully recovered to the number observed in the IAA-treated wild-type plants, as has been observed in many of the ABA biosynthetic and signaling mutants (Brady et al., 2003). This would be because the *MYB96*-mediated ABA signals also exert its role in an auxin-independent manner or because

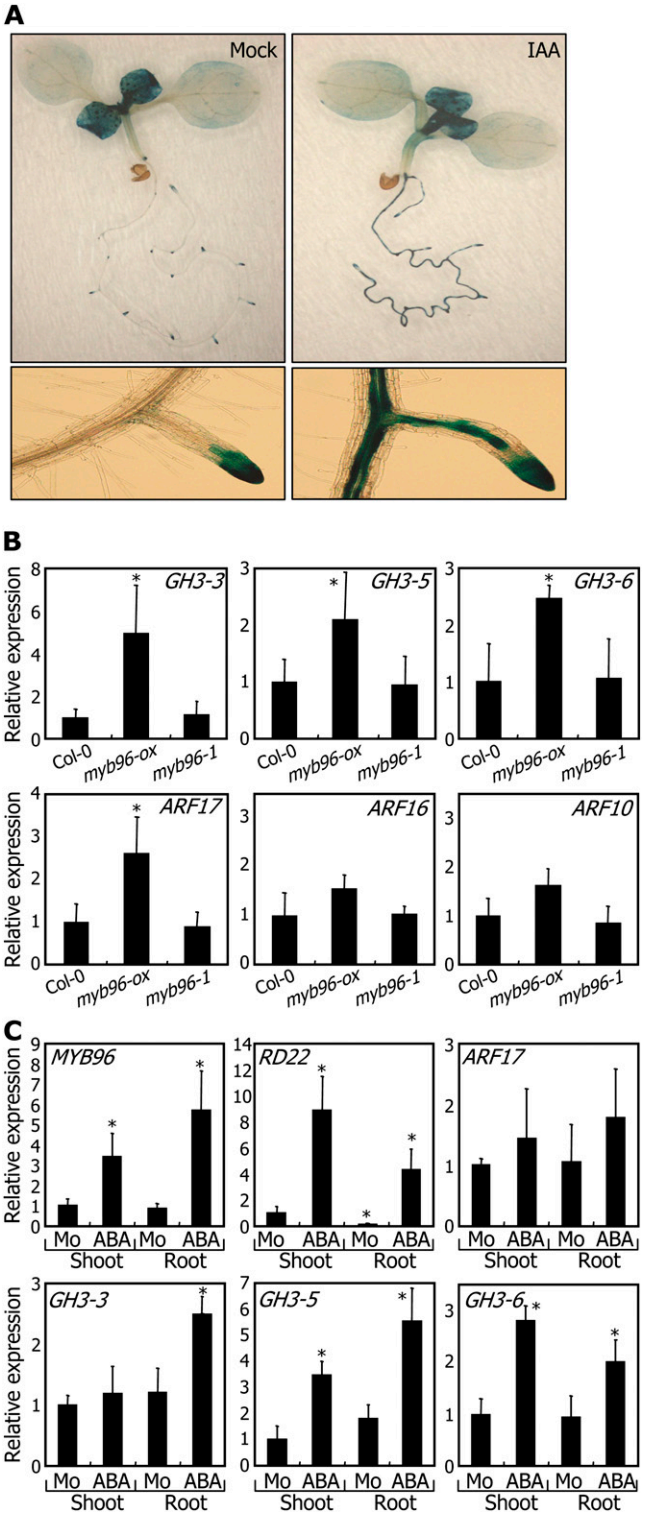

Figure 5. *MYB96* is induced by IAA primarily in the roots. Transcript levels were determined as described in Figure 1F. A, Effects of IAA on *MYB96* expression in the roots. Two-week-old transgenic plants expressing the *pMYB96-GUS* fusion were incubated in MS liquid cultures supplemented with 10 μM IAA for 12 h and subjected to GUS staining. B, Transcript levels of auxin-responsive genes. Two-week-old whole plants grown on MS agar plates were used for RNA extraction. Error bars represent SE (*t* test; * $P < 0.01$). C, Effects of ABA on expression of auxin-responsive genes. Two-week-old wild-type plants grown on MS agar plates were incubated for 6 h in MS liquid cultures supplemented with 20 μM ABA before harvesting plant materials. Mo, Mock. Error bars represent SE (*t* test; * $P < 0.01$).

endogenous auxin levels are adjusted to a certain degree by the elevated GH3 activities in the *myb96-ox* mutant (see below). These observations indicate that the *MYB96*-mediated ABA signals are, at least in part, integrated into an auxin signaling pathway that involves a few *GH3* genes. Meanwhile, the effects of IAA on primary root growth in the *myb96-ox* and *myb96-1* mutants were similar to those in the wild-type roots (Fig. 6D), indicating that the *MYB96*-mediated auxin signaling is specific to lateral root formation.

MYB96 Regulates Lateral Root Growth

Our data indicated that *MYB96* regulates lateral root development as well as drought resistance by modulating ABA signals. Consistent with this notion, the root phenotype of the *myb96-ox* mutant was quite similar to that observed in wild-type plants grown in the presence of ABA. Both plants exhibited normal primary root growth but with fewer lateral roots (Fig. 7A). In addition, *MYB96* expression was initiated in the lateral root primordia after developmental stage III (Supplemental Fig. S11).

Interestingly, light microscope-assisted counting of the lateral roots and lateral root primordia revealed that although visible lateral roots were reduced in the *myb96-ox* mutant, more lateral root primordia were observed in the mutant (Fig. 7B; Laplaze et al., 2007). Furthermore, total numbers of lateral roots and lateral root primordia were similar in the wild type and *myb96-ox* roots. We also found that lateral root length was significantly shorter in the *myb96-ox* mutant but slightly longer in the *myb96-1* mutant (Fig. 7C). These observations indicate that *MYB96* regulates later steps of lateral root development but does not affect earlier developmental steps, such as lateral root initiation.

Differential interference contrast microscopy further supported the role of *MYB96* in lateral root development. In wild-type roots, most of the lateral root primordia were expanded through cell divisions after emergence, and a meristem tissue consisting of smaller cells was visible within the tips of lateral roots (Fig. 7D), indicative of lateral root meristem activation (Malamy and Benfey, 1997; Malamy, 2005). In the *myb96-ox* mutant, lateral root primordia were normally developed, but further lateral root growth was suppressed, as was observed in the ABA-treated wild-type roots (Fig. 7D; Supplemental Fig. S12). Together, our data strongly support that *MYB96* regulates the activation of lateral root meristem and lateral root growth. This view is also consistent with the ABA-mediated repression of the activation of newly

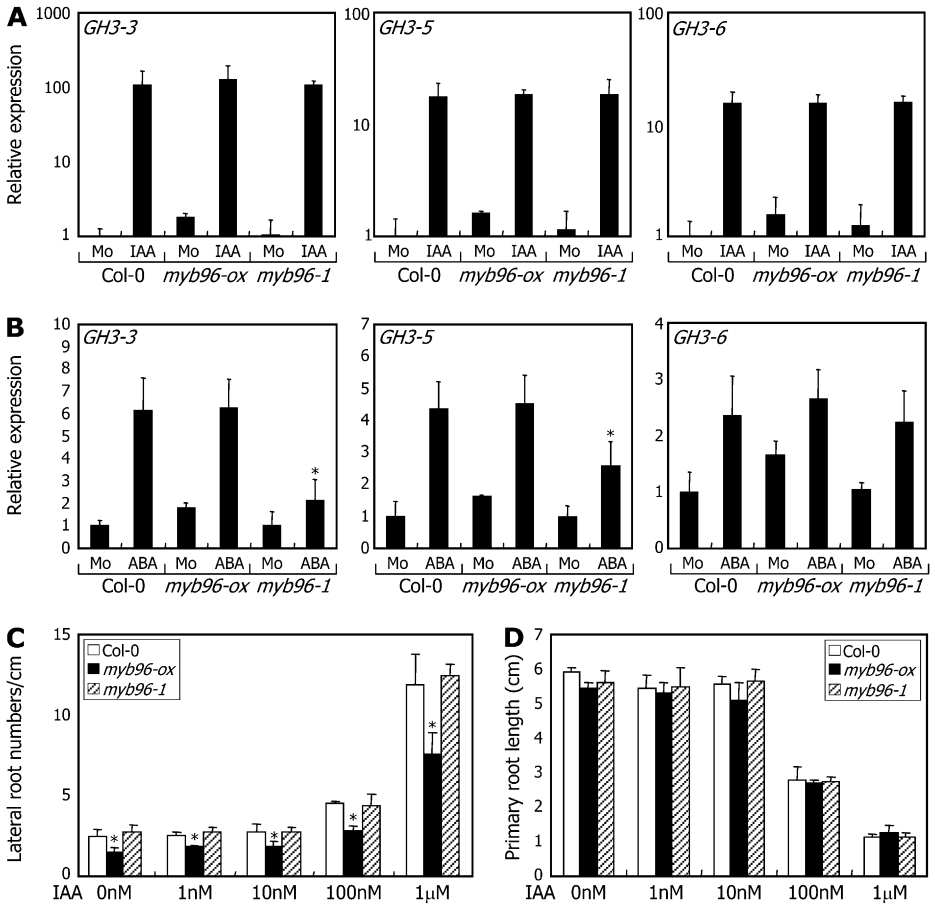

Figure 6. *MYB96*-mediated ABA signals are related to auxin. In A and B, transcript levels were determined as described in Figure 1F. Mo, Mock. A, Effects of IAA on expression of auxin-responsive genes in *myb96-ox* and *myb96-1*. Two-week-old whole plants grown on MS agar plates were incubated in MS liquid cultures supplemented with 20 μM IAA for 6 h before harvesting root samples. The *y* axis is presented on a logarithmic scale for better comparison of fold changes in the first three graphs. B, Effects of ABA on expression of *GH3* genes in the roots. Two-week-old plants grown on MS agar plates were incubated in MS liquid cultures supplemented with 20 μM ABA for 6 h before harvesting root samples. Error bars represent SE (*t* test; * $P < 0.01$). C, Effects of IAA on lateral root formation. Plants were grown on vertical MS agar plates supplemented with 0 to 1 μM IAA for 3 weeks, and visible lateral root numbers were counted. Twenty seedlings were counted and averaged. Error bars represent SE (*t* test; * $P < 0.01$). D, Effects of IAA on primary root growth. Measurements were carried out using 2-week-old plants grown on MS agar plates as described in C.

established lateral root meristems (De Smet et al., 2003).

Expression analysis of the genes involved in lateral root development also supported the role of *MYB96* in lateral root meristem activation and lateral root growth. Expression of *ABI3* and *ABI5*, which mediate ABA signaling during lateral root meristem activation (Brocard et al., 2002; Brocard-Gifford et al., 2004), was induced in the *MYB96*-overexpressing *myb96-ox* mutant but reduced in the knockout *myb96-1* mutant (Fig. 7E). *NCED9*, which encodes an ABA biosynthetic enzyme functioning in lateral root formation (Taylor et al., 2000), also showed similar expression patterns in the *myb96-ox* and *myb96-1* mutants. In contrast, *CYCB1;1* and *KRP2*, which regulate cell cycling during earlier steps of lateral root formation (Wang et al., 1998; Himanen et al., 2002; Verkest et al., 2005), were unaffected in the mutants. These observations demonstrate that *MYB96* mediates ABA signals in regulating the activation of lateral root meristem.

Endogenous Auxin Levels Are Altered in *myb96-ox*

We found that *MYB96*-mediated ABA signals are incorporated into an auxin signaling pathway that involves *GH3-3* and *GH3-5* genes, suggesting that the levels of endogenous auxins would be altered in the *myb96-ox* mutant.

To examine this possibility, we employed the DR5-GUS reporter containing an auxin-inducible, synthetic DR5 promoter fused to the GUS-coding sequence, which is frequently used as a marker for auxin responses (Ulmasov et al., 1997). We crossed the *myb96-ox* mutant with the transgenic plants expressing the DR5-GUS reporter. The GUS activity was evidently reduced in the lateral roots as well as in the vasculature of the primary roots in the *myb96-ox* background (Fig. 7F). The *GUS* transcript level was also lower in the mutant roots (Fig. 7G). To confirm these results, we measured the levels of endogenous auxins in the *myb96-ox* mutant. The level of conjugated IAA forms were approximately two times higher in the *myb96-ox* mutant (Fig. 7H), which is consistent with the induction of *GH3-3* and *GH3-5* genes in the mutant (Fig. 6A). Meanwhile, the level of free IAA was unaltered to a discernible degree in the mutant, which would be due to rigorous control of auxin homeostasis under stress conditions (Dombrecht et al., 2007; Park et al., 2007).

In accordance with *MYB96* regulation of the *GH3-3* and *GH3-5* genes, distribution of GUS activity in the roots of the transgenic plants expressing the *pGH3-5/*

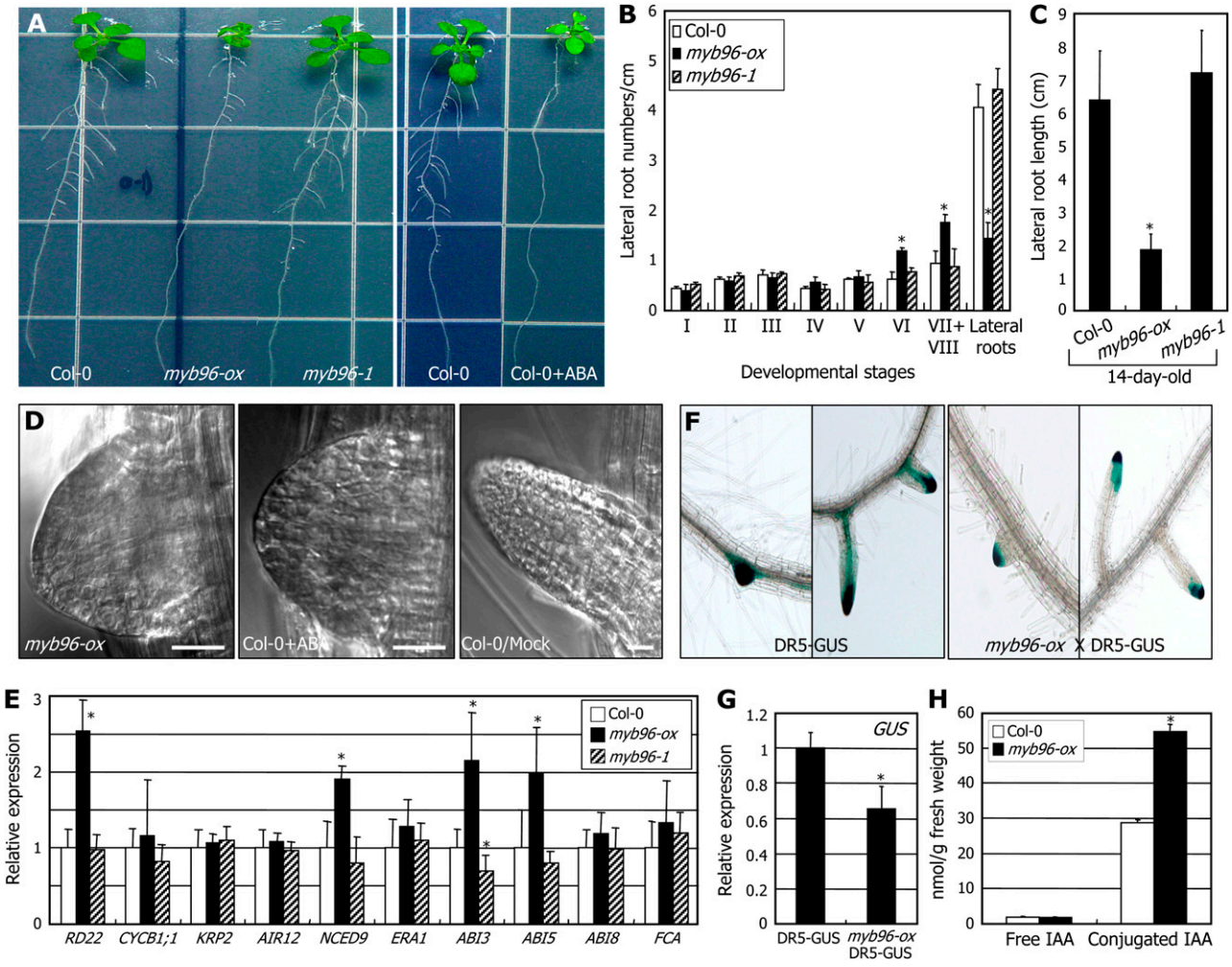

Figure 7. *MYB96* regulates lateral root growth. A, Comparison of lateral root formation of *myb96-ox* and ABA-treated wild-type plants. Seedlings were germinated and grown on MS agar plates for 2 weeks (left). For ABA treatments, seedlings grown at 22°C for 3 d on MS agar plates after cold imbibition were transferred to MS agar plates supplemented with 1 μM ABA and further grown for 2 weeks (right). B, Counting of lateral root primordia using a light microscope. Thirty plants at each growth stage were counted and averaged. Error bars represent SE (*t* test; * $P < 0.01$). C, Lateral root lengths of *myb96-ox* and *myb96-1*. Lengths of lateral roots on 20 plants grown on vertical MS agar plates for 3 weeks were measured and averaged. Error bars represent SE (*t* test; * $P < 0.01$). D, Suppression of lateral root growth right after emergence in *myb96-ox*. Plants were grown at 22°C for 3 d on MS agar plates after cold imbibition and further grown for 2 weeks either in the presence or absence of 1 μM ABA. Lateral root primordia were compared by differential interference contrast microscopy. Bar = 50 μm. E, Expression of lateral root development-related genes in *myb96-ox* and *myb96-1*. Transcript levels were determined as described in Figure 1F using root samples. Error bars represent SE (*t* test; * $P < 0.01$). F and G, Measurements of GUS activity. The DR5-GUS reporter construct was transformed into wild-type plants (DR5-GUS) and the *myb96-ox* mutant (*myb96-ox* × DR5-GUS). Two-week-old roots were subjected to GUS staining (F). *GUS* expression was quantitated by qRT-PCR using root samples (G). Error bars represent SE (*t* test; * $P < 0.01$). H, Measurements of endogenous auxin contents. Extraction and quantification of endogenous auxins were carried out using whole plants grown for 3 weeks on MS agar plates. Measurements of five independent plant samples, each with 0.5 g of fresh whole plants, were averaged. Error bars represent SE (*t* test; * $P < 0.01$).

WES1-GUS reporter was very similar to that observed in the roots of the *pMYB96-GUS* transgenic plants (Supplemental Fig. S13). The *GH3-5/WES1* expression was localized primarily in the lateral root primordium, like the *MYB96* expression. In addition, whereas ABA up-regulated *GH3-5* expression mainly in the lateral root primordium, IAA induced its expression throughout the whole roots.

Altogether, our data demonstrate that *MYB96* is a critical component of ABA signaling that mediates plant responses to drought stress via *RD22* (Fig. 8). The *MYB96*-mediated ABA signals are also incorporated into an auxin signaling pathway that probably involves a subset of *GH3* genes. The signaling cross talk between ABA and auxin is a key part of molecular mechanisms governing lateral root meristem activa-

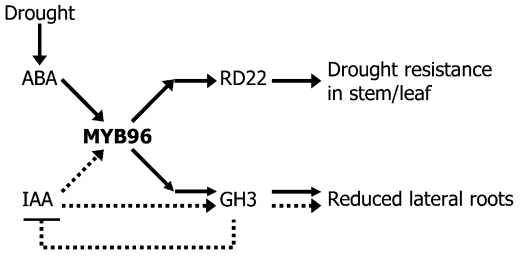

Figure 8. *MYB96* mediates ABA signals via *RD22* in regulating drought stress response. The *MYB96*-mediated ABA signals also induce *GH3* genes to regulate lateral root development under drought conditions. This signaling pathway is probably linked to the *GH3*-mediated negative feedback loop maintaining auxin homeostasis (Park et al., 2007). The solid arrows indicate ABA signal transduction, and the dotted arrows indicate auxin signal transduction.

tion under drought conditions. However, it is evident that the *MYB96-GH3* signaling cascade is not directly related to the *RD22*-mediated ABA signaling pathway functioning in the drought resistance response of the shoots.

DISCUSSION

MYB96-Mediated ABA Signaling in Drought Resistance

Among the approximately 200 MYB proteins in the Arabidopsis genome, up to 126 members belong to the R2R3-type subfamily (Yanhui et al., 2006). The roles of the R2R3-type MYB members have been demonstrated in a variety of developmental processes, such as development of meristem, flowers, and seeds (Schmitz et al., 2002; Zhang et al., 2007; Petroni et al., 2008), cell cycle control (Araki et al., 2004), and stomatal closure (Liang et al., 2005). Some MYB members also regulate plant responses to biotic and abiotic stress conditions (Abe et al., 2003; Raffaele et al., 2008; Van der Ent et al., 2008).

In this work, we demonstrated that a R2R3-type MYB transcription factor, MYB96, modulates an ABA signaling pathway that helps regulate plant responses to drought stress. The knockout *myb96-1* mutant is susceptible to drought. The stomatal apertures of the knockout mutant were not evidently different from those of wild-type plants when grown under normal growth conditions. In contrast, the stomatal apertures decreased to a lesser degree in the mutant than in wild-type plants. Furthermore, the drought sensitivity of the mutant was efficiently rescued by the expression of a wild-type *MYB96* gene in the mutant, showing that *MYB96*-mediated ABA signals induce plant resistance responses to water deficit by reducing stomatal opening.

Suppression of lateral root development is a typical adaptive response of plants to drought stress. Lateral roots are significantly reduced in the *myb96-ox* mutant, and the root phenotype is hypersensitive to ABA, demonstrating that *MYB96* regulates later steps of lateral root development under drought stress conditions.

At first glance, it seems paradoxical that primary root growth is either unaffected or even enhanced, but lateral root formation is suppressed, when soil water is limited. However, this is conceivable if we consider what plants require to survive under drought conditions. By sacrificing lateral root formation, stem growth, and leaf expansion as well as metabolic activity, primary root growth can be maintained and thus the underground water reached (Deak and Malamy, 2005; Malamy, 2005). The shade avoidance response in plants may be a similar such strategy. Plants growing in shade put most of their available metabolic energy into maintaining primary stem growth to reach the light that is essential for photosynthesis (Morelli and Ruberti, 2000).

It has been suggested that reduced lateral root formation might be caused by suppression of lateral root meristem activation, not by reduced initiation of lateral roots (Deak and Malamy, 2005; Malamy, 2005). We also observed that the number of lateral root primordia in the *myb96-ox* root was similar to that in the wild-type root. In contrast, the lateral root meristem activation was suppressed in the mutant. It is evident, therefore, that *MYB96* regulates primarily the later steps of lateral root development, such as establishment and activation of lateral root meristem. This notion is also consistent with previous observations (De Smet et al., 2003; Deak and Malamy, 2005) showing that drought suppresses lateral root formation when lateral root primordia reach the developmental stage consisting of three to five cell layers.

Mutants with altered lateral root development differentially respond to drought stress (Deak and Malamy, 2005; Xiong et al., 2006), supporting the close relationship between drought responses and lateral root development. Drought-mediated suppression of lateral root development is widely accepted to be an adaptive response to ensure plant survival under unfavorable growth conditions. In this view, the lateral root response is considered to be a determinant of drought tolerance as well as a mechanism for drought resistance (Xiong et al., 2006).

However, some caution should be used in interpreting the data. While the *MYB96*-overexpressing *myb96-ox* mutant had significantly reduced lateral roots, the *myb96-1* mutation has only marginal effects on lateral root development. This might be attributable to functional redundancy of multiple MYB transcription factors and/or of multiple drought stress signaling pathways governing lateral root development. Nevertheless, we believe that *MYB96* is likely a critical component of such adaptive responses under drought conditions. First, whereas primary root growth was unaffected, the lateral roots were reduced in the *myb96-ox* mutant, which is similar to the root phenotypes observed in plants grown under drought stress conditions (Deak and Malamy, 2005; Malamy, 2005). Second, *MYB96* expression is initiated and localized

specifically in developing lateral root primordia, and it is further elevated by ABA. Furthermore, it has been widely documented that lateral root development is intimately related to plant responses to drought. The *myb96-ox* mutant exhibited enhanced resistance to drought with reduced lateral roots.

ABA-Auxin Cross Talk in Adaptive Responses to Drought

Symptoms frequently observed in plants exposed to biotic and abiotic stress conditions include reduction of growth and metabolism and alteration of plant architecture and morphology. These would be due to reallocation of metabolic resources between different physiological processes to optimize plant survival under unfavorable growth conditions (Heil and Baldwin, 2002; Jackson et al., 2004). Accordingly, signaling cross talk between auxin and ABA or salicylic acid has been extensively documented. An example is the functional relationship between auxin and ABA in lateral root development under drought conditions.

While auxin plays a promotive role throughout lateral root developmental steps, ABA modulates auxin responses and signaling primarily at later steps of lateral root development (De Smet et al., 2003; Deak and Malamy, 2005). Experimental evidence obtained in recent years also supports the signaling cross talk between auxin and ABA (Suzuki et al., 2001; Brady et al., 2003). However, the underlying molecular schemes have not yet been elucidated.

Our data demonstrate that *MYB96* regulates ABA-mediated drought stress signals during lateral root development. Of particular interest is the fact that ABA affects an auxin signaling pathway that involves a subset of *GH3* genes. The *GH3* genes encode enzymes that conjugate amino acids, such as Leu, Ala, Asp, and Glu, to IAA (Staswick et al., 2002, 2005). Several members of the *GH3* genes are rapidly induced by auxin. Therefore, it has been suggested that the rapid up-regulation of *GH3* genes by auxin may help to maintain the appropriate level of endogenous auxin (Staswick et al., 2005; Park et al., 2007).

We found that expression of the *GH3* genes was elevated in the *myb96-ox* mutant. Drought and ABA treatments also elevated the level of the *GH3* transcripts, particularly in the lateral root primordia. These observations suggest that ABA-mediated drought stress signals modulate the roles of auxin by inducing *GH3* enzyme genes, ultimately reducing lateral root formation. Supporting this notion, the level of conjugated auxins was elevated in the *myb96-ox* mutant, although the level of free auxin was unaltered. This view is also supported by a previous report showing that endogenous IAA levels were significantly reduced in the roots of hydroponic tomato (*Solanum lycopersicum*) cultures exposed to high salinity (Normanly, 1997). Furthermore, the phenotypes of the *myb96-ox* mutant are quite similar to those of the Arabidopsis mutants overexpressing *GH3* genes, such as *DFL1* and *WES1* (Nakazawa et al., 2001; Park et al., 2007), in that both mutants exhibit dwarfed growth with reduced lateral roots.

We believe that the regulation of the *GH3* signaling pathway by *MYB96*-mediated ABA signals is important for lateral root formation, although expression of *GH3* genes and endogenous levels of active IAA were unaltered in the *myb96-1* mutant, based on the following observations. First, *GH3-3* and *GH3-5* genes are induced, particularly in the roots, by ABA and drought in a *MYB96*-dependent manner. Second, endogenous levels of conjugated IAA forms are higher by approximately 2-fold in the *MYB96*-overexpressing *myb96-ox* mutant. No changes in the levels of free IAA in the mutant probably result from the fact that whole plants were used for measurements of auxin contents. In an assay using the DR5-GUS reporter, lower GUS activity was detected in the *myb96-ox* roots.

Our data support that *MYB96* functions as a molecular link that interconnects ABA and auxin signals in lateral root development, which provides a fitness adaptation to drought stress (Heil and Baldwin, 2002). Meanwhile, we found that the *GH3* genes were also induced by auxin independent of *MYB96*. This would be related to the regulation of auxin homeostasis by *GH3-5/WES1* and other *GH3* genes functioning under biotic and abiotic stress conditions (Park et al., 2007). It seems that there would be multiple signaling pathways governing auxin metabolism, each exerting its role under distinct environmental conditions. Alternatively, the *GH3*-mediated signaling pathway would be further modulated by some tissue-specific factors, such as *MYB96* in lateral root formation, in different plant tissues.

MATERIALS AND METHODS

Plant Materials and Growth Conditions

All Arabidopsis (*Arabidopsis thaliana*) lines used were in the ecotype Col-0, unless otherwise specified. Plants were grown in a controlled culture room at 22°C with a relative humidity of 60% under long-day conditions (16 h of light and 8 h of dark) with white light illumination (120 μmol photons m^{-2} s^{-1}) provided by fluorescent FLR40D/A tubes (Osram).

Isolation of *myb96-ox* and *myb96-1*

Ecotype Col-0 was transformed with the activation-tagging vector pSKI015 that contains the CaMV 35S enhancer element (Weigel et al., 2000). To select herbicide-resistant transformants, T0 seeds were collected, sown in soil, and sprayed twice a week with a 1:1,000 dilution (in water) of Finale solution (AgrEvo) containing 5.78% Basta. A morphogenic mutant (*myb96-ox*) with dwarfed growth and curled leaves was chosen for further analysis. The *myb96-1* knockout mutant was isolated from a pool of T-DNA insertion lines (GABI_120B05) deposited in the Nottingham Arabidopsis Stock Centre at the University of Nottingham. Absence of *MYB96* gene expression in the mutant was verified by reverse transcription (RT)-PCR before use.

The single T-DNA insertion event in the *myb96-ox* mutant was verified by genomic Southern-blot hybridization using the 35S enhancer sequence as a probe, followed by analysis of segregation ratios. The flanking sequences of the T-DNA insertion site were determined by thermal asymmetric interlaced-PCR (Liu et al., 1995).

For the *MYB96* complementation test, a genomic clone containing the *MYB96* gene with its own promoter (approximately 2.1 kb) was subcloned

into the promoterless pKGWFS7 Gateway vector (Invitrogen). The PCR primers used for genomic PCR were 5′-AAAAAGCAGGCTCGCACCATAAATAATCATAACTTTATCAT-3′ (forward) and 5′-AGAAAGCTGGGTTTCTGTTTTCACCTTTTGATGAG-3′ (reverse). The expression construct was transformed into the *myb96-1* knockout mutant.

Analysis of Transcript Levels

Quantitative real-time (qRT)-PCR was employed for measuring transcript levels. RNA sample preparation, reverse transcription, and quantitative PCR were carried out based on the rules that have recently been proposed by Udvardi et al. (2008) to ensure reproducible and accurate measurements. Extraction of total RNA samples from appropriate plant materials and RT-PCR conditions have been described previously (Kim et al., 2006). The RNA samples were extensively pretreated with RNAse-free DNAse to eliminate any contaminating genomic DNA. The PCR primers used are listed in Supplemental Table S1.

qRT-PCR was carried out in 96-well blocks with an Applied Biosystems 7500 Real-Time PCR System using the SYBR Green I Master Mix in a volume of 25 μL. The PCR primers were designed using Primer Express Software installed into the system and listed in Supplemental Table S1. The two-step thermal cycling profile used was 15 s at 94°C and 1 min at 68°C. An *eIF4A* gene (At3g13920) was included in the assays as an internal control for normalizing the variations in cDNA amounts used (Gutierrez et al., 2008). The qRT-PCRs were carried out in biological triplicates using RNA samples extracted from three independent plant materials grown under identical growth conditions. The comparative $\Delta\Delta C_T$ method was used to evaluate the relative quantities of each amplified product in the samples. The threshold cycle (C_T) was automatically determined for each reaction by the system set with default parameters. The specificity of the PCR was determined by melt curve analysis of the amplified products using the standard method installed in the system.

Treatments with Growth Hormones and Abiotic Stresses

Two-week-old plants grown on MS agar plates were transferred to MS liquid cultures supplemented with various growth hormones, including IAA, mJA, and ACC (10 μM each, unless otherwise specified), for the indicated time periods, and plant materials were harvested for RNA extraction. ABA was used at a final concentration of either 1 or 5 μM for MS agar plates or 20 μM for MS liquid cultures.

For the assays on the effects of drought on gene expression, 2-week-old plants grown on MS agar plates were put on dry 3MM paper and incubated at room temperature for the indicated time periods. For the assays on the effects of high salinity on gene expression, 2-week-old plants grown on MS agar plates were soaked in MS liquid cultures containing 200 mM NaCl and incubated under constant light for the indicated time periods. For cold treatments, 2-week-old plants grown on MS agar plates were transferred to a cold chamber set at −7°C and incubated for the indicated time periods before harvesting plant materials. Whole plants were used for RNA extraction unless otherwise specified.

Drought stress was induced in 2-week-old plants in soil (grown in 36-cm^3 soil pots) by halting watering. To prevent direct air drying of seedlings, small pores were made in the plastic cover 7 d following the start of drought, and the cover was removed 7 d later. Watering was reinitiated after 20 d, and survival rates were calculated for each group of plants. Three independent measurements of 30 seedlings were averaged.

Effects of ABA on Lateral Root Formation

To examine the effects of ABA on lateral root formation and primary root growth, seedlings were grown at 22°C for 3 d under long days on MS agar plates after cold imbibition and transferred to MS agar plates supplemented with appropriate concentrations of ABA. They were further grown for 2 weeks before counting lateral root numbers and measuring lengths of lateral roots and primary roots. Lateral root primordia were counted with the aid of a light microscope. Thirty countings or measurements were averaged for each assay.

Water Loss Assays

The fourth to seventh leaves were detached from 4-week-old plants and put on 3MM paper at room temperature for the indicated time periods, and fresh weights of the leaves were measured, as described previously (Jung et al., 2008), using a Sartorius Analytical Balance with a readability of 0.01 mg (DE/CP-225D). Leaves from seven plants were measured and averaged.

Confocal Microscopy and Differential Interference Contrast Microscopy

To examine the developmental steps of lateral root formation, the roots of 2-week-old plants grown on MS agar plates were mounted on a slide glass and monitored using differential interference contrast optics on a Carl Zeiss confocal microscope (LSM510) as described previously (Malamy and Benfey, 1997).

Subcellular Localization of MYB96 and Histological Assays

The GFP-coding sequence was fused in frame to the 3′ end of the *MYB96* gene sequence, and the gene fusion was subcloned into the pBA002 vector (Kost et al., 1998) for transient expression in onion (*Allium cepa*) epidermal cells. After incubation for 24 h at 22°C, the cells were subjected to bright-field and fluorescence microscopy.

For histochemical analysis of the GUS activity, the seedlings or plants were incubated in 90% acetone for 20 min on ice, washed twice with rinsing solution [50 mM sodium phosphate, pH 7.2, 0.5 mM $K_3Fe(CN)_6$, and 0.5 mM $K_4Fe(CN)_6$], and subsequently incubated at 37°C for 18 to 24 h in rinsing solution containing 2 mM 5-bromo-4-chloro-3-indolyl-β-D-glucuronide (Duchefa). The seedlings were then incubated in a series of ethanol solutions ranging from 15% to 80% in order to remove chlorophylls from plant tissues. They were then mounted on microscope slides and visualized using a Nikon SMZ 800 microscope.

Measurements of Endogenous Auxin Contents

Plants were grown on MS agar plates for 3 weeks. Approximately 0.5 g of whole plants was used for each measurement. Extraction and quantification of endogenous contents of free IAA and conjugated IAA forms were carried out essentially as described previously (Prinsen et al., 2000). Plant materials were frozen in liquid nitrogen and extracted with 80% ethanol. [Indole-D_5]IAA (Cambridge Isotopes) was added to the plant materials as an internal standard immediately before the extraction. The lipid substances were allowed to be precipitated by incubating for 16 h at −20°C. The precipitates and debris were removed by centrifugation (17,600*g*, 10 min, 4°C). For determination of total IAA, the ethanol extract was subjected to alkaline hydrolysis by boiling in 1 N NaOH. The IAAs in the extract were pretreated with a C_{18} cartridge (Waters) and separated on a reverse-phase column (Apollo C18, 5 μm; Alltech) connected to a HPLC system (600E; Waters) equipped with a fluorescence detector (486; Waters). The IAA peaks were monitored with the emission at 360 nm (excitation at 286 nm). The purified IAAs were concentrated and derivatized with (trimethylsilyl) diazomethane. The IAAs were finally resolved on a capillary gas chromatography column (FactorFour VF-5ms; Varian) set on a gas chromatography-mass spectrometry system (CP 3000, Saturn 2200; Varian). The fragmentation peak of 130 was compared with that of 135 from the internal standard and used for quantification. Five measurements were averaged.

Sequence data from this article can be found in the GenBank/EMBL data libraries under accession numbers *MYB96* (At5g62470), *RD22* (At5g25610), *GH3-3* (*DFL1*, At2g23170), *GH3-5* (*WES1*, At4g27260), and *GH3-6* (At5g54510).

Supplemental Data

The following materials are available in the online version of this article.

Supplemental Figure S1. Effects of ABA on primary root growth.

Supplemental Figure S2. Amino acid sequence and domain structure of the MYB96 protein.

Supplemental Figure S3. Transcript levels of abiotic stress genes and ABA-related genes in the presence of 20 μM ABA.

Supplemental Figure S4. Stomatal density.

Supplemental Figure S5. Effects of auxin and ABA on tissue-specific expression of *MYB96*.

Supplemental Figure S6. Effects of auxin on *MYB96* expression in the primary root.

Supplemental Figure S7. Expression of genes involved in auxin responses and signaling.

Supplemental Figure S8. Growth stage-dependent expression of *MYB96*.

Supplemental Figure S9. Kinetic comparison of ABA effects on *ARF17* and *GH3-5* expression.

Supplemental Figure S10. Effects of IAA on *RD22* expression and transcript levels of *RD22* in *wes-1D* and *wes1-1*.

Supplemental Figure S11. Developmental stage-dependent expression of *MYB96* in lateral root primordia.

Supplemental Figure S12. Effects of ABA on lateral root formation in wild-type plants.

Supplemental Figure S13. Effects of IAA and ABA on expression of *MYB96* and *WES1*.

Supplemental Table S1. Primers used in this work.

ACKNOWLEDGMENT

We thank Dr. D. Weigel for kindly providing the pSKI015 vector.

Received July 2, 2009; accepted July 17, 2009; published July 22, 2009.

LITERATURE CITED

Abe H, Urao T, Ito T, Seki M, Shinozaki K, Yamaguchi-Shinozaki K (2003) *Arabidopsis* AtMYC2 (bHLH) and AtMYB2 (MYB) function as transcriptional activators in abscisic acid signaling. Plant Cell **15:** 63–78

Araki S, Ito M, Soyano T, Nishihama R, Machida Y (2004) Mitotic cyclins stimulate the activity of c-Myb-like factors for transactivation of G2/M phase-specific genes in tobacco. J Biol Chem **279:** 32979–32988

Brady SM, Sarkar SF, Bonetta D, McCourt P (2003) The *ABSCISIC ACID INSENSITIVE3* (*ABI3*) gene is modulated by farnesylation and is involved in auxin signaling and lateral root development in *Arabidopsis*. Plant J **34:** 67–75

Brocard IM, Lynch TJ, Finkelstein RR (2002) Regulation and role of the *Arabidopsis abscisic acid-insensitive 5* gene in abscisic acid, sugar, and stress response. Plant Physiol **129:** 1533–1543

Brocard-Gifford I, Lynch TJ, Garcia ME, Malhotra B, Finkelstein RR (2004) The *Arabidopsis thaliana ABSCISIC ACID-INSENSITIVE8* encodes a novel protein mediating abscisic acid and sugar responses essential for growth. Plant Cell **16:** 406–421

Casimiro I, Beeckman T, Graham N, Bhalerao R, Zhang H, Casero P, Sandberg G, Bennett MJ (2003) Dissecting *Arabidopsis* lateral root development. Trends Plant Sci **8:** 165–171

Celenza JL Jr, Grisafi PL, Fink GR (1995) A pathway for lateral root formation in *Arabidopsis thaliana*. Genes Dev **9:** 2131–2142

Deak KI, Malamy J (2005) Osmotic regulation of root system architecture. Plant J **43:** 17–28

De Smet I, Signora L, Beeckman T, Inze D, Foyer CH, Zhang H (2003) An abscisic acid-sensitive checkpoint in lateral root development of *Arabidopsis*. Plant J **33:** 543–555

De Smet I, Vassileva V, De Rybel B, Levesque MP, Grunewald W, Van Damme D, Van Noorden G, Naudts M, Van Isterdael G, De Clercq R, et al (2008) Receptor-like kinase ACR4 restricts formative cell divisions in the *Arabidopsis* root. Science **322:** 594–597

De Smet I, Zhang H, Inze D, Beeckman T (2006) A novel role for abscisic acid emerges from underground. Trends Plant Sci **11:** 434–439

Dombrecht B, Xue GP, Sprague SJ, Kirkegaard JA, Ross JJ, Reid JB, Fitt GP, Sewelam N, Schenk PM, Manners JM, et al (2007) MYC2 differentially modulates diverse jasmonate-dependent functions in *Arabidopsis*. Plant Cell **19:** 2225–2245

Dubrovsky JG, Doerner PW, Colón-Carmona A, Rost TL (2000) Pericycle cell proliferation and lateral root initiation in Arabidopsis. Plant Physiol **124:** 1648–1657

Dubrovsky JG, Sauer M, Napsucialy-Mendivil S, Ivanchenko MG, Friml J, Shishkova S, Celenza J, Benková E (2008) Auxin acts as a local morphogenetic trigger to specify lateral root founder cells. Proc Natl Acad Sci USA **105:** 8790–8794

Gubler F, Millar AA, Jacobsen JV (2005) Dormancy release, ABA and pre-harvest sprouting. Curr Opin Plant Biol **8:** 183–187

Gutierrez L, Mauriat M, Guénin S, Pelloux J, Lefebvre JF, Louvet R, Rusterucci C, Moritz T, Guerineau F, Bellini C, et al (2008) The lack of a systematic validation of reference genes: a serious pitfall undervalued in reverse transcription-polymerase chain reaction (RT-PCR) analysis in plants. Plant Biotechnol J **6:** 609–618

Heil M, Baldwin IT (2002) Fitness costs of induced resistance: emerging experimental support for a slippery concept. Trends Plant Sci **7:** 61–67

Himanen K, Boucheron E, Vanneste S, Engler JA, Inze D (2002) Auxin-mediated cell cycle activation during early lateral root initiation. Plant Cell **14:** 2339–2351

Horvath DP, Anderson JV, Chao WS, Foley ME (2003) Knowing when to grow: signals regulating bud dormancy. Trends Plant Sci **8:** 534–540

Ivanchenko MG, Muday GK, Dubrovsky JG (2008) Ethylene-auxin interactions regulate lateral root initiation and emergence in *Arabidopsis thaliana*. Plant J **55:** 335–347

Jackson MW, Stinchcombe JR, Korves TM, Schmitt J (2004) Costs and benefits of cold tolerance in transgenic *Arabidopsis thaliana*. Mol Ecol **13:** 3609–3615

Jung C, Seo JS, Han SW, Koo YJ, Kim CH, Song SI, Nahm BH, Choi YD, Cheong JJ (2008) Overexpression of *AtMYB44* enhances stomatal closure to confer abiotic stress tolerance in transgenic Arabidopsis. Plant Physiol **146:** 623–635

Kim YS, Kim SG, Park JE, Park HY, Lim MH, Chua NH, Park CM (2006) A membrane-bound NAC transcription factor regulates cell division in *Arabidopsis*. Plant Cell **18:** 3132–3144

Kost B, Spielhofer P, Chua NH (1998) A GFP-mouse talin fusion protein labels plant actin filaments in vivo and visualizes the actin cytoskeleton in growing pollen tubes. Plant J **16:** 393–401

Laplaze L, Benkova E, Casimiro I, Maes L, Vanneste S, Swarup R, Weijers D, Calvo V, Parizot B, Herrera-Rodriguez MB, et al (2007) Cytokinins act directly on lateral root founder cells to inhibit root initiation. Plant Cell **19:** 3889–3900

Liang YK, Dubos C, Dodd IC, Holroyd GH, Hetherington AM, Campbell MM (2005) AtMYB61, an R2R3-MYB transcription factor controlling stomatal aperture in *Arabidopsis thaliana*. Curr Biol **15:** 1201–1206

Little DY, Rao H, Oliva S, Daniel-Vedele F, Krapp A, Malamy JE (2005) The putative high-affinity nitrate transporter NRT2.1 represses lateral root initiation in response to nutritional cues. Proc Natl Acad Sci USA **102:** 13693–13698

Liu YG, Mitsukawa N, Oosumi T, Whittier RF (1995) Efficient isolation and mapping of *Arabidopsis thaliana* T-DNA insert junctions by thermal asymmetric interlaced PCR. Plant J **8:** 457–463

Ljung K, Hul AK, Kowalczyk M, Marchant A, Celenza J, Cohen JD, Sandberg G (2002) Biosynthesis, conjugation, catabolism and homeostasis of indole-3-acetic acid in *Arabidopsis thaliana*. Plant Mol Biol **49:** 249–272

Malamy JE (2005) Intrinsic and environmental response pathways that regulate root system architecture. Plant Cell Environ **28:** 67–77

Malamy JE, Benfey PN (1997) Organization and cell differentiation in lateral roots of *Arabidopsis thaliana*. Development **124:** 33–44

Malamy JE, Ryan KS (2001) Environmental regulation of lateral root initiation in Arabidopsis. Plant Physiol **127:** 899–909

Mallory AC, Bartel DP, Bartel B (2005) MicroRNA-directed regulation of *Arabidopsis AUXIN-RESPONSE FACTOR17* is essential for proper development and modulates expression of early auxin response genes. Plant Cell **17:** 1360–1375

Morelli G, Ruberti I (2000) Shade avoidance responses: driving auxin along lateral routes. Plant Physiol **122:** 621–626

Nakazawa M, Yabe N, Ichikawa T, Yamamoto YY, Yoshizumi T, Hasunuma K, Matsui M (2001) *DFL1*, an auxin-responsive *GH3* gene homologue, negatively regulates shoot cell elongation and lateral root formation, and positively regulates the light response of hypocotyl length. Plant J **25:** 213–221

Normanly J (1997) Auxin metabolism. Physiol Plant **100:** 431–442

Park JE, Park JY, Kim YS, Staswick PE, Jeon J, Yun J, Kim SY, Kim J, Lee

YH, Park CM (2007) *GH3*-mediated auxin homeostasis links growth regulation with stress adaptation response in *Arabidopsis*. J Biol Chem **282:** 10036–10046

Petroni K, Falasca G, Calvenzani V, Allegra D, Stolfi C, Fabrizi L, Altamura MM, Tonelli C (2008) The *AtMYB11* gene from *Arabidopsis* is expressed in meristematic cells and modulates growth in planta and organogenesis *in vitro*. J Exp Bot **59:** 1201–1213

Prinsen E, van Laer S, Öden S, van Onckelen H (2000) Auxin analysis. *In* G Tucker, JA Oberts, eds, Plant Hormone Protocols. Humana Press, Totowa, NJ, pp 49–65

Raffaele S, Vailleau F, Léger A, Joubès J, Miersch O, Huard C, Blée E, Mongrand S, Domergue F, Roby D (2008) A MYB transcription factor regulates very-long-chain fatty acid biosynthesis for activation of the hypersensitive cell death response in *Arabidopsis*. Plant Cell **20:** 752–767

Schmitz G, Tillmann E, Carriero F, Fiore C, Theres K (2002) The tomato *Blind* gene encodes a MYB transcription factor that controls the formation of lateral meristems. Proc Natl Acad Sci USA **99:** 1064–1069

Sorin C, Bussell JD, Camus I, Ljung K, Kowalczyk M, Geiss G, McKhann H, Garcion C, Vaucheret H, Sandberg G, et al (2005) Auxin and light control of adventitious rooting in *Arabidopsis* require ARGONAUTE1. Plant Cell **17:** 1343–1359

Staswick PE, Serban B, Rowe M, Tiryaki I, Maldonado MT, Maldonado MC, Suza W (2005) Characterization of an *Arabidopsis* enzyme family that conjugates amino acids to indole-3-acetic acid. Plant Cell **17:** 616–627

Staswick PE, Tiryaki I, Rowe ML (2002) Jasmonate response locus *JAR1* and several related *Arabidopsis* genes encode enzymes of the firefly luciferase superfamily that show activity on jasmonic, salicylic, and indole-3-acetic acids in an assay for adenylation. Plant Cell **14:** 1405–1415

Stracke R, Werber M, Weisshaar B (2001) The *R2R3-MYB* gene family in *Arabidopsis thaliana*. Curr Opin Plant Biol **4:** 447–456

Suzuki M, Kao CY, Cocciolone S, McCarty DR (2001) Maize VP1 complements *Arabidopsis abi3* and confers a novel ABA/auxin interaction in roots. Plant J **28:** 409–418

Tan BC, Joseph LM, Deng WT, Liu L, Li QB, Cline K, McCarty DR (2003) Molecular characterization of the *Arabidopsis* 9-*cis* epoxycarotenoid dioxygenase gene family. Plant J **35:** 44–56

Taylor IB, Burbidge A, Thompson AJ (2000) Control of abscisic acid synthesis. J Exp Bot **51:** 1563–1574

Udvardi MK, Czechowski T, Scheible WR (2008) Eleven golden rules of quantitative RT-PCR. Plant Cell **20:** 1736–1737

Ulmasov T, Murfett J, Hagen G, Guilfoyle TJ (1997) Aux/IAA proteins repress expression of reporter genes containing natural and highly active synthetic auxin response elements. Plant Cell **9:** 1963–1971

Van der Ent S, Verhagen BW, Van Doorn R, Bakker D, Verlaan MG, Pel MJ, Joosten RG, Proveniers MC, Van Loon LC, Ton J, et al (2008) MYB72 is required in early signaling steps of *rhizobacteria*-induced systemic resistance in Arabidopsis. Plant Physiol **146:** 1293–1304

Verkest A, Weinl C, Inzé D, De Veylder L, Schnittger A (2005) Switching the cell cycle: Kip-related proteins in plant cell cycle control. Plant Physiol **139:** 1099–1106

Wang H, Qi Q, Schorr P, Cutler AJ, Crosby WL, Fowke LC (1998) ICK1, a cyclin-dependent protein kinase inhibitor from *Arabidopsis thaliana* interacts with both Cdc2a and CycD3, and its expression is induced by abscisic acid. Plant J **15:** 501–510

Weigel D, Ahn JH, Blázquez MA, Borevitz JO, Christensen SK, Fankhauser C, Ferrándiz C, Kardailsky I, Malancharuvil EJ, Neff MM, et al (2000) Activation tagging in Arabidopsis. Plant Physiol **122:** 1003–1013

Xie Q, Frugis G, Colgan D, Chua NH (2000) *Arabidopsis* NAC1 transduces auxin signal downstream of TIR1 to promote lateral root development. Genes Dev **14:** 3024–3036

Xie Q, Guo HS, Dallman G, Fang S, Weissman AM, Chua NH (2002) SINAT5 promotes ubiquitin-related degradation of NAC1 to attenuate auxin signals. Nature **12:** 167–170

Xiong L, Wang RG, Mao G, Koczan JM (2006) Identification of drought tolerance determinants by genetic analysis of root response to drought stress and abscisic acid. Plant Physiol **142:** 1065–1074

Yamaguchi-Shinozaki K, Shinozaki K (1993) The plant hormone abscisic acid mediates the drought-induced expression but not the seed-specific expression of *rd22*, a gene responsive to dehydration stress in *Arabidopsis thaliana*. Mol Gen Genet **238:** 17–25

Yanhui C, Xiaoyuan Y, Kun H, Meihua L, Jigang L, Zhaofeng G, Zhiqiang L, Yunfei Z, Xiaoxiao W, Xiaoming Q, et al (2006) The MYB transcription factor superfamily of *Arabidopsis*: expression analysis and phylogenetic comparison with the rice MYB family. Plant Mol Biol **60:** 107–124

Yu H, Chen X, Hong YY, Wang Y, Xu P, Ke SD, Liu HY, Zhu JK, Oliver DJ, Xiang CB (2008) Activated expression of an *Arabidopsis* HD-START protein confers drought tolerance with improved root system and reduced stomatal density. Plant Cell **20:** 1134–1151

Zhang Y, Yang C, Li Y, Zheng N, Chen H, Zhao Q, Gao T, Guo H, Xie Q (2007) SDIR1 is a RING finger E3 ligase that positively regulates stress-responsive abscisic acid signaling in *Arabidopsis*. Plant Cell **19:** 1912–1929